Geomechanics and Engineering, *Vol. 24, No. 2 (2021) 167-178*
DOI: https://doi.org/10.12989/gae.2021.24.2.167

Reliability analysis of strip footing under rainfall using KL-FORM

Suozhu Fei[1a], Xiaohui Tan*[1], Wenping Gong[2b], Xiaole Dong[1c], Fusheng Zha[1d] and Long Xu[1e]

[1]*School of Resources and Environmental Engineering, Hefei University of Technology, Hefei 230009, China*
[2]*Faculty of Engineering, China University of Geosciences, Wuhan, Hubei 430074, China*

(Received July 15, 2020, Revised November 26, 2020, Accepted January 8, 2021)

Abstract. Spatial variability is an inherent uncertainty of soil properties. Current reliability analyses generally incorporate random field theory and Monte Carlo simulation (MCS) when dealing with spatial variability, in which the computational efficiency is a significant challenge. This paper proposes a KL-FORM algorithm to improve the computational efficiency. In the proposed KL-FORM, Karhunen-Loeve (KL) expansion is used for discretizing random fields, and first-order reliability method (FORM) is employed for reliability analysis. The KL expansion and FORM can be used in conjunction, through adopting independent standard normal variables in the discretization of KL expansion as the basic variables in the FORM. To illustrate the effectiveness of this KL-FORM, it is applied to a case study of a strip footing in spatially variable unsaturated soil under rainfall, in which the bearing capacity of the footing is computed by numerical simulation. This case study shows that the KL-FORM is accurate and efficient. The parametric analyses suggest that ignoring the spatial variability of the soil may lead to an underestimation of the reliability index of the footing.

Keywords: spatial variability; Karhunen-Loeve expansion; first-order reliability analysis; footing; rainfall

1. Introduction

Many footings have been built in unsaturated soils. Rainfall infiltration will affect the distribution of matric suction and bearing capacity of unsaturated soils (Qi *et al.* 2019). Knowledge pertaining to variation of the stability of a footing with time is essential for accurate assessment and design of a footing. Spatial variabilities of soil parameters also affect the stability of a footing. In recent years, influences of the spatial variabilities of soil properties on the performance of geotechnical systems, such as foundations and slopes (Cho and Park 2010, Cheon and Gilbert 2014, Gong *et al.* 2016, Lombardi *et al.* 2017), have received considerable attention.

Spatial variability is also known as spatial autocorrelation, which means that soil properties at one point are correlated to those at nearby points. An effective tool for describing the spatial variability of soil parameters is random field theory, in which the spatial variability or autocorrelation is often expressed by the autocorrelation function (ACF) (Vanmarcke 1977, Moshtaghin 2016, Fei *et al.* 2019). An ACF models the reduction in autocorrelation with the distance between two points and this reduction can be characterized by the autocorrelation distance (ACD). When the spatial variabilities of soil parameters are considered within the reliability analysis of geotechnical systems, numerical simulations such as the finite element method (FEM) or finite difference method (FDM) are often required to compute the value of the performance function, due to the fact that different values of the soil properties can be much easily assigned to different locations at the study site within the numerical simulation. In the context of the random FEM or FDM, a continuous random field is usually discretized into discrete random variables at different spatial points before they are mapped onto finite element or finite difference grids as input parameters to the numerical modeling.

Many methods have been proposed for the discretization of random fields, and they can be classified into three main categories: point discretization methods (e.g., the midpoint and nodal point method) (Stefanou 2009), average-type discretization methods (e.g., the local average and weighted integral methods) (Deodatis 1991, Vanmarcke and Grigoriu 1983), and series expansion methods (e.g., the Karhunen-Loeve (KL) and wavelet expansion methods) (Montoya *et al.* 2019, Sudret and Kiureghian 2000). Among these methods, the KL expansion method is quite suitable for discretizing cross-correlated non-Gaussian random variables; as an outcome, the KL expansion is widely applied for probabilistic analysis in geotechnical systems with spatially variable soils (Phoon *et al.* 2005, Schueller and Jensen 2008).

After a random field is discretized into a sequence of random variables at different discrete points, MCS is

*Corresponding author, Professor
E-mail: tanxh@hfut.edu.cn
[a]Ph.D. Student
E-mail: fsz2017@mail.hfut.edu.cn
[b]Professor
E-mail: wenpinggong@cug.edu.cn
[c]Ph.D. Student
E-mail: dongxiaole@mail.hfut.edu.cn
[d]Professor
E-mail: geozha@hfut.edu.cn
[e]Associate Professor
E-mail: xulong_2005@hfut.edu.cn

ISSN: 2005-307X (Print), 2092-6219 (Online)

usually used for the stochastic simulation of system response of geotechnical systems (Cho and Park 2010, Le *et al.* 2015, Liu *et al.* 2017, Gong *et al.* 2018, Al-Bittar *et al.* 2018, Mouyeaux *et al.* 2018). Although MCS is simple and easy to apply, it is computationally inefficient when the system response is calculated through numerical simulation. This is because a huge number of numerical simulations are required for obtaining the reliability index or failure probability of a geotechnical system. To overcome this shortcoming, Subset Simulation (SS) is employed to perform the reliability analysis for geo-structures with spatially various soils. SS is an advanced Monte Carlo Simulation which can improve the efficiency of generating failure samples in MCS. (Santoso *et al.* 2011, Jiang and Huang 2016, Liu *et al.* 2017). However, it still requires several thousand calls of the deterministic numerical simulation (Li *et al.* 2016, Jiang and Huang 2016). Another approach for the reliability analysis considering soil's spatial variability is probabilistic collocation method (Li *et al.* 2009, Jiang *et al.* 2014), in which the system response is expressed by polynomial chaos expansions (PCEs), and the coefficients in the PCEs are determined by solving the equations for a set of carefully selected collocation points. Similar to SS method, the probabilistic collocation method still requires at least several thousand calls of the deterministic numerical simulation for obtaining the reliability index accurately (Jiang *et al.* 2014). Ji *et al.* (2018) presented a simplified Hasofer-Lind-Rackwitz-Fiessler iterative algorithm for FORM, and applied this FORM algorithm in the reliability analysis of earth slope with spatially variable soils. In their case study, the point discretization method and the autocorrelated slices method were combined to model the spatial variation of soil properties along a specific slip surface. However, if a numerical method is required for the calculation of the performance function, this FORM algorithm is hard to handle the analysis situation where too many random variables are involved.

To improve computational efficiency when analyzing the spatial variability in geotechnical engineering, a KL-FORM algorithm will be developed in this study. In this new KL-FORM algorithm, the KL is adopted for the discretization of random fields and the FORM is employed to perform reliability analysis. The application process, accuracy and efficiency of the proposed method will be illustrated through the reliability analysis of a strip footing with spatially variable unsaturated soil properties under rainfall infiltration. Benefiting from the computational efficiency of the proposed method, parametric analyses can be easily performed, which can enable the detail investigation of the factors that influence the time-variant reliability index of the footing under rainfall. The proposed method is introduced in Section 2, followed by a case study of a strip foundation and discussions in Section 3. They are followed with the summary and concluding remarks in Section 4.

2. Methodology

2.1 Discretization of random field using KL expansion

2.1.1 Theory of random field

Spatial variability of soil properties can be described using random field theory. In a random field, the value of a variable at one point is correlated to the values at nearby points. The spatial variability or autocorrelation of soil properties can be represented by an ACF, which models the reduction in autocorrelation with the distance between two points. Several ACFs have been presented to characterize the spatial variability of soil properties; among which, the squared exponential function (SQX) is widely used (Jha and Ching 2013, Rackwitz 2000):

$$\rho(\boldsymbol{x}_1, \boldsymbol{x}_2) = \exp\left[-(|x_{11} - x_{21}|/L_{\mathrm{h}})^2 - (|x_{12} - x_{22}|/L_{\mathrm{v}})^2\right] \quad (1)$$

Another commonly used ACF is the single exponential function (SNX), which is expressed as follows:

$$\rho(\boldsymbol{x}_1, \boldsymbol{x}_2) = \exp(-|x_{11} - x_{21}|/L_{\mathrm{h}} - |x_{12} - x_{22}|/L_{\mathrm{v}}) \quad (2)$$

where ρ is the autocorrelation coefficient between two points ($\boldsymbol{x}_1$ and $\boldsymbol{x}_2$); x_{i1} and x_{i2} are the coordinate components of points $\boldsymbol{x}_i$ along the horizontal and vertical directions, respectively; and L_{h} and L_{v} are autocorrelation distances (ACDs) along the horizontal and vertical directions, respectively.

The soil properties between any two spatial points vary due to the spatial variability of soils. A smaller ACD value indicates that the soil properties vary greatly in space, whereas a larger ACD value indicates that the soil properties are strongly correlated within a large range (Stefanou 2009). In the traditional probabilistic or reliability analysis using random variable method, soil properties in a soil layer are considered to be the same, implying that the ACD is infinite large and all soil property values are perfectly correlated.

2.1.2 KL expansion method

The KL expansion method can be used for simulation of both homogeneous and non-homogeneous stochastic fields. It is a special case of the orthogonal series expansion method where the orthogonal functions are the eigenfunctions of a Fredholm integral equation of the second kind with the autocovariance function as kernel (Cho and Park 2010, Stefanou 2009, Phoon *et al.* 2004, Zhang and Ellingwood 1994). Denote the cross-correlation coefficient matrix of N random fields in the original random space as $\boldsymbol{R}_{\mathrm{X}}$ (the size of $\boldsymbol{R}_{\mathrm{X}}$ is $N \times N$). If the ith (i = 1, …, N) random field is a normal random field, the discrete value at point $\boldsymbol{x}$ can be expressed as follows (Cho and Park 2010, Phoon *et al.* 2002, Sachdeva *et al.* 2007):

$$\hat{H}_i(\boldsymbol{x}) = \mu_{X_i} + \sigma_{X_i} \hat{H}_i^D(\boldsymbol{x}) = \mu_{X_i} + \sigma_{X_i} \sum_{j=1}^{M} \sqrt{\lambda_j}\, f_j(\boldsymbol{x})(\boldsymbol{\xi}\boldsymbol{L}^{\mathrm{T}})_{ji} \quad (3)$$

In addition, if the ith random field is a lognormal random field, the expression for the discrete value at point $\boldsymbol{x}$ is as follows:

$$\hat{H}_i(\boldsymbol{x}) = \exp\left(\mu_{\ln X_i} + \sigma_{\ln X_i} \hat{H}_i^D(\boldsymbol{x})\right) = \exp\left(\mu_{\ln X_i} + \sigma_{\ln X_i} \sum_{j=1}^{M} \sqrt{\lambda_j}\, f_j(\boldsymbol{x})(\boldsymbol{\xi}\boldsymbol{L}^{\mathrm{T}})_{ji}\right) \quad (4)$$

where $\hat{H}_i^{\mathrm{D}}(\boldsymbol{x})$ is the discrete standard normal random field and is independent of the mean ($\mu_{\mathrm{X}i}$) and standard deviation

(σ_{Xi}) of random field X_i; $\hat{H}_i(\boldsymbol{x})$ is the final discrete result whose value is affected by the values of μ_{Xi} and σ_{Xi}; $\mu_{\ln Xi}$ and $\sigma_{\ln Xi}$ are the mean and the standard deviation of the logarithm of random field X_i; M is the number of series expansion terms; λ_j (j=1, 2, …, M) is the jth largest value of eigenvalues and $f_j(\boldsymbol{x})$ is the jth eigenfunction of the ACF $\rho(\boldsymbol{x}_1, \boldsymbol{x}_2)$; $\boldsymbol{\xi}$ is a matrix of standard normal random variables of size $M \times N$; $\boldsymbol{L}$ is a lower triangular matrix that is a Cholesky decomposition of cross-correlation matrix $\boldsymbol{R}_Y$ in dependent normal space, and $\boldsymbol{R}_Y$ can be computed from the cross-correlation matrix $\boldsymbol{R}_X$ in the original random space (Cho and Park 2010, Tan *et al.* 2017); and $\boldsymbol{L}^T$ means the transposition of matrix $\boldsymbol{L}$. The product of matrix $\boldsymbol{\xi}$ and matrix $\boldsymbol{L}^T$ can be denoted as matrix $\boldsymbol{\chi}$ (i.e., $\boldsymbol{\chi} = \boldsymbol{\xi}\boldsymbol{L}^T$), which is a random matrix that considers the cross-correlation of N random fields.

2.1.3 Estimation of discrete error

The number of series expansion terms (M) in Eqs. (3) and (4) should theoretically be infinite large. To reduce the computation effort of random field discretization, M is generally assumed to be a small value. This simplification results in a discrete error of the KL expansion method. For the selection of a proper value of M, the discrete error must be estimated (Li *et al.* 2009, Sachdeva *et al.* 2007, Laloy *et al.* 2013). As suggested by Sudret and Kiureghian (2000), the mean value of point-wise discrete errors can be used to indicate the global accuracy of the discretization. The formula for the mean discrete error (ε_d) is as follows:

$$\varepsilon_d = \frac{1}{N_e}\sum_{j=1}^{N_e}\varepsilon(\boldsymbol{x}_j) = \frac{1}{N_e}\sum_{j=1}^{N_e}\left(1-\sum_{i=1}^{M}\lambda_i f_i^2(\boldsymbol{x}_j)\right) \quad (5)$$

where $\varepsilon(\boldsymbol{x}_j)$ is the point-wise discrete error at point $\boldsymbol{x}_j$; and N_e is the number of discrete points. After the mean discrete error is estimated using Eq. (5), the optimal number of expansion terms (M) can be selected by comparing ε_d with a predefined allowable discrete error (ε_{d0}). The number of series expansion terms with ε_d closest to but smaller than ε_{d0} is selected as the optimal value of the number of expansion terms.

2.1.4 Main steps of the KL expansion method

As a whole, the KL expansion method for discretizing random fields can be divided into three parts.

Part 1: Calculate the eigenvalue (λ), eigenfunction ($f(\boldsymbol{x})$), discrete error, and number of series expansion terms. The autocorrelation of soil properties is considered in the calculation of the values of λ and $f(\boldsymbol{x})$. The detail computation formulas of λ and $f(\boldsymbol{x})$ can refer to Sudret and Kiureghian (2000), Phoon *et al.* (2005), Sachdeva *et al.* (2007), and Cho and Park (2010).

Part 2: Generate the matrixes $\boldsymbol{\xi}$ and $\boldsymbol{\chi}$. The matrix $\boldsymbol{\xi}$ in Eq. (3) or Eq. (4) is composed of N columns of independent standard normal variables, and each standard normal variable is composed of M random values. The matrix $\boldsymbol{\chi} = \boldsymbol{\xi}\boldsymbol{L}^T$ can reflect the cross-correlation of N random fields because the matrix $\boldsymbol{L}$ is a decomposition of the cross-correlation matrix $\boldsymbol{R}_Y$. If there is no cross-correlation between N random fields, matrixes $\boldsymbol{\xi}$ and $\boldsymbol{\chi}$ are equal.

Part 3: Calculate the discrete standard normal random field ($\hat{H}_i^D(\boldsymbol{x})$) and the final discrete random field ($\hat{H}_i(\boldsymbol{x})$) using Eq. (3) or (4).

Note that the generation of matrix $\boldsymbol{\xi}$ in Part 2 does not depend on the results of Part 1. The value of matrix $\boldsymbol{\xi}$ can be generated randomly or in a specific way. If the KL expansion method is a subprogram of another program, matrix $\boldsymbol{\xi}$ can be considered as an input variable whose value is computed in the main program. Inspired by this idea, a KL-FORM is proposed for the reliability analysis of geotechnical systems with spatially variable soils.

2.2 Reliability analysis using KL-FORM

A key step in the KL expansion method is the generation of the random matrix $\boldsymbol{\xi}$ with consideration that $\boldsymbol{\xi}$ is composed of N columns of independent standard normal variables. Matrix $\boldsymbol{\xi}$ can be generated randomly. Therefore, MCS is widely used for reliability analysis after a random field is discretized by the KL expansion (Cho and Park 2010). Although MCS is easy to realize, it needs huge computation efforts. This might hinder the application of random field theory in engineering applications.

To improve the computational efficiency, we propose a KL-FORM for the reliability analysis with spatially variable soil properties. In the KL-FORM algorithm, the KL expansion is adopted for discretizing random fields, and the FORM is employed for reliability analysis. After the KL expansion, N random fields can be discretized into a sequence of discrete values that are controlled by the random matrix $\boldsymbol{\xi}$ of size $M \times N$, or alternatively, by $n = M \times N$ standard normal variables (see Eqs. (3) or (4)). By considering these standard normal variables as basic variables (i.e., $\boldsymbol{X} = [X_1, X_2, \ldots, X_n]$), the traditional FORM can be adopted to carry out reliability analysis. Because the number of series expansion terms M is usually small (Li *et al.* 2009, Sachdeva *et al.* 2007), the value of n for N random fields is also small. Therefore, the KL-FORM algorithm with a limited number of random variables is computationally efficient. The flowchart of the proposed KL-FORM algorithm is summarized in Fig. 1.

In Fig. 1, the left column of the flow chart represents the main steps of the traditional FORM. The calculation of the reliability index (β) is an iterative process. The initial value ($\boldsymbol{x}_0$) for the design point $\boldsymbol{x}^*$ is usually set as the mean value of variable $\boldsymbol{X}$, which corresponds to an initial value of $\beta = 0$. After setting the value of the design point $\boldsymbol{x}^*$ for the kth iteration, the value of the performance function (Z) and the gradient of the performance function with respect to the basic variable $\boldsymbol{X}$ (i.e., $\partial Z/\partial \boldsymbol{X}$) at the design point needs to be calculated. Then, the new reliability index and design point for the kth iteration can be obtained. If the absolute value of the difference between the reliability indices of the two consecutive iterative computations is less than a predefined tolerance ε_β, the iterative computation stops; otherwise, the iterative computation continues. Any existing computer programs or software using the FORM can be adopted as the left side in Fig. 1 for the calculation of the reliability index. Interested readers are suggested to refer Tan and Wang (2009), Ji and Kodikara (2015) and Ji *et al.* (2018) for details of the FORM algorithm.

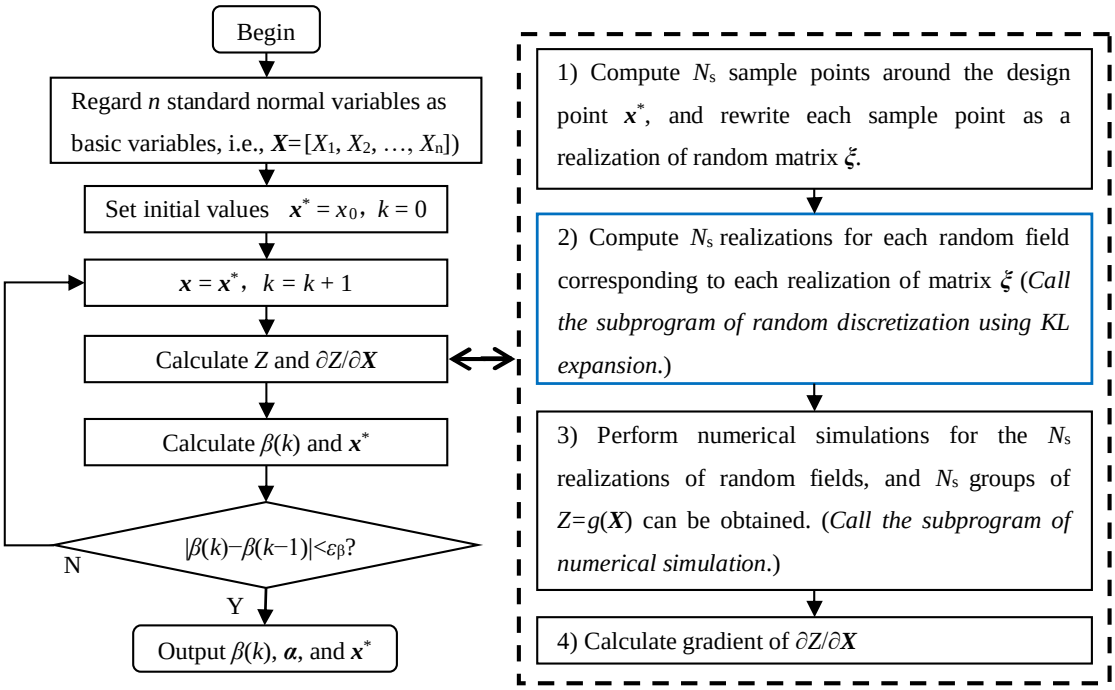

Fig. 1 Flow chart of the KL-FORM algorithm

As shown in Fig. 1, the main task of the FORM is to calculate the value of performance function (Z) and its gradient $\partial Z/\partial \boldsymbol{X}$ at design point $\boldsymbol{x}^*$. When the performance function is implicit, numerical simulations are required for computing the value of Z, and a numerical differentiation method such as central difference method (CDM) is needed for computing the gradient $\partial Z/\partial \boldsymbol{X}$. The equation used to calculate $\partial Z/\partial X_i$ using the CDM at design point $\boldsymbol{x}^*$ is as follows (Duncan 2000):

$$\frac{\partial Z}{\partial X_i}=\frac{Z(x_1^*,...,x_{i-1}^*,x_i^*+\sigma_{X_i},x_{i+1}^*,...,x_n^*)-Z(x_1^*,...,x_{i-1}^*,x_i^*-\sigma_{X_i},x_{i+1}^*,...,x_n^*)}{2\sigma_{X_i}} \quad (6)$$

Note that one sample point (x_1^*, …, x_{i-1}^*, x_i^*, x_{i+1}^*, …, x_n^*) is needed for the calculation of Z, and two sample points ((x_1^*, …, x_{i-1}^*, $x_i^*+\sigma_{Xi}$, x_{i+1}^*, …, x_n^*) and (x_1^*, …, x_{i-1}^*, $x_i^*-\sigma_{Xi}$, x_{i+1}^*, …, x_n^*)) are needed for the calculation of $\partial Z/\partial X_i$ (i = 1, 2, …, n). Therefore, the calculation of Z and $\partial Z/\partial \boldsymbol{X}$ for each iteration of the KL-FORM algorithm requires $2n$+1 sample points.

The right column of the flow chart in Fig. 1 shows the process for calculating the performance function (Z) and its gradient with respect to basic variable ($\partial Z/\partial \boldsymbol{X}$) at design point $\boldsymbol{x}^*$. It is composed of four steps.

Step 1: Compute $N_s = 2n+1 = 2MN+1$ sample points around the design point $\boldsymbol{x}^*$ according to Eq. (6), and rewrite each sample point as a realization of the random matrix $\boldsymbol{\xi}$. For example, if the number of random fields is N = 2, then, the number of random variables is $n = M \times N = 2M$, and the design point is (x_1^*, …, x_M^*, x_{M+1}^*, …, x_{2M}^*). The corresponding relationship between the sample point $\boldsymbol{x}^*$and the random matrix $\boldsymbol{\xi}$ is

$$\boldsymbol{x}^*=[x_1^*,...,x_M^*,x_{M+1}^*,...,x_{2M}^*]\Rightarrow\boldsymbol{\xi}=\begin{bmatrix}x_1^* & x_{M+1}^*\\ \vdots & \vdots\\ x_M^* & x_{2M}^*\end{bmatrix} \quad (7)$$

Step 2: Compute N_s realizations for each random field corresponding to each realization of the matrix $\boldsymbol{\xi}$. This step is not required in the traditional FORM, and it is a special step for the KL-FORM algorithm. In this step, the discretization of each random field at the $N_s = 2MN+1$ sample points needs the calling of a subprogram of random discretization using the KL expansion. Considering the N_s groups of random matrixes $\boldsymbol{\xi}$ generated in Step 1 as the input variables of the subprogram of the KL expansion method, N_s groups of discrete random fields can be computed.

Step 3: Calculate values of the implicit performance function at N_s sample points. A subprogram of numerical simulation is required for the calculation of values of the implicit performance function in this step. Any standalone deterministic numerical packages can be adopted to calculate the performance function. The N_s numerical simulations make this the most time-consuming step in the KL-FORM algorithm.

Step 4: Calculate the gradient of performance function with respect to the basic variable ($\partial Z/\partial \boldsymbol{X}$) at design point $\boldsymbol{x}^*$. After values of the performance function at N_s sample points have been calculated, the value of $\partial Z/\partial \boldsymbol{X}$ can be easily obtained using Eq. (6).

It should be mentioned that although the left side of the flow chart for the KL-FORM algorithm in Fig. 1 is the same as the traditional FORM algorithm, the basic variable $\boldsymbol{X}$ has different meanings in this new method. In the traditional FORM, $\boldsymbol{X}$ is a random vector that is composed of N random variables, and each random variable has its own probabilistic distribution and statistics. In the proposed KL-FORM algorithm, the basic variable $\boldsymbol{X}$ is composed of $n = M \times N$ independent standard normal variables, where M is the number of series expansion terms, and N is the number of random fields. Although there is no correlation among the n components of random variable $\boldsymbol{X}$ in the proposed KL-

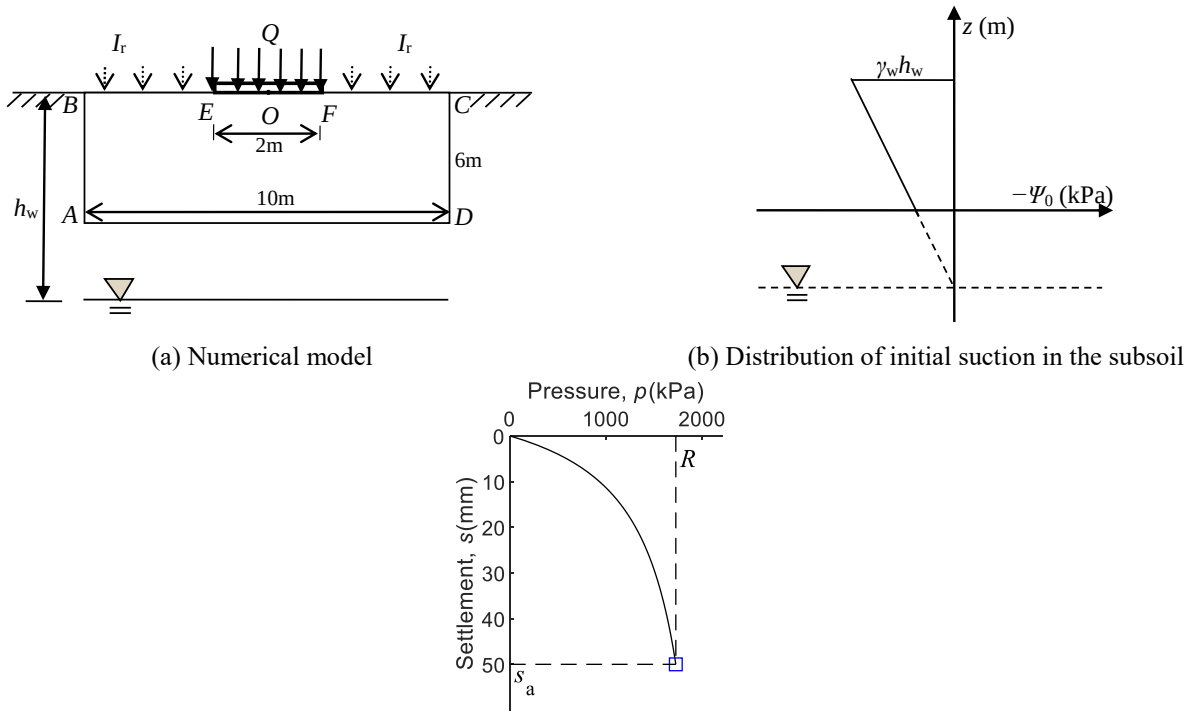

(a) Numerical model

(b) Distribution of initial suction in the subsoil

(c) *p-s* relationship

Fig. 2 Numerical model of a strip footing and the distribution of initial suction in the subsoil

Table 1 Parameters of unsaturated soil

Description	Parameters	Value	Description	Parameters	Value
Effective cohesion	c' (kPa)	50.0	van Genuchten parameter	a_V (kPa)	14.6
Effective angle of friction	φ' (°)	25.0	van Genuchten parameter	n_V	1.26
Elastic modulus	E (MPa)	25.7	van Genuchten parameter	m_V	0.21
Poisson's radio	μ	0.29	Saturated hydraulic conductivity	k_s (mm/d)	60

Table 2 Iterative process using the KL-FORM algorithm for the basic computation condition

No.	Number of sample points	Coordinates of design points	Reliability index	Runtime (s)
0	0	0, 0, 0, 0, 0, 0, 0, 0	0	0
1	17	0.51, -0.49, 0.26, 0.00, 1.02, -0.94, 0.43, 0.00	1.64	18.56
2	17	1.05, -1.07, 0.62, 0.00, 1.38, -1.36, 0.71, 0.00	2.63	18.36
3	17	1.31, -1.38, 0.86, 0.00, 1.20, -1.23, 0.69, 0.00	2.79	18.10
4	17	1.36, -1.45, 0.94, 0.00, 1.07, -1.11, 0.65, 0.00	2.76	18.25
5	17	1.36, -1.46, 0.95, 0.00, 1.05, -1.10, 0.64, 0.00	2.76	17.81

FORM algorithm, both the cross-correlation of different random fields and the autocorrelation of each random field can be considered in the process of random discretization.

3. Illustrative example—a strip footing under rainfall infiltration

3.1 Parameters setting

A shallow strip footing with width B = 2 m is located on the surface of an unsaturated soil (Fig. 2). A rainfall intensity (I_r = 60 mm/d) acts on the surface of the unsaturated soil for three days. The depth of the groundwater level is h_w = 10 m. A constant pressure of Q = 400 kPa is acting at the bottom of the footing, and the allowable settlement is s_a = 50 mm.

The mechanical parameters (effective cohesion c' and effective angle of friction φ'), deformation parameters (elastic module E and Poisson's ratio μ), and hydraulic parameters (curve-fitting parameters of soil-water characteristic curve using van Genuchten model (Fredlund and Houston 2009, van Genuchten 1980, Le *et al.* 2015), i.e., a_v, n_v, m_v, and k_s) for the unsaturated soil are listed in Table 1. Like Cho and Park (2010), the two shear strength parameters (c' and φ') are considered as stationary normal random fields, while the other parameters are regarded as constants. The coefficients of variation (COVs) of c' and φ' are 0.3 and 0.2, respectively. The spatial variability of these two soil parameters is represented by the squared exponential ACF (Eq. (1)). Several authors have reported that the horizontal ACD is much larger than the vertical ACD (Cho and Park 2010, Gui *et al.* 2000, Ahmed 2009). It is widely considered that the vertical ACD (L_v) usually focuses on a small range of 0.5-4 m, while the horizontal ACD (L_h) can vary within a very large range (Cho and Park 2010, Ahmed 2009, Phoon and Kulhawy 1999).

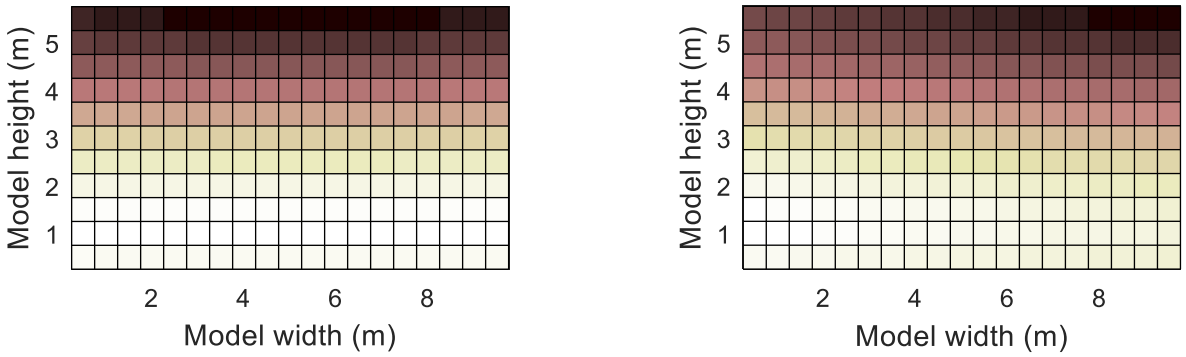

(a) Random field of c' (b) Random field of φ'

Fig. 3 Discretization of random fields

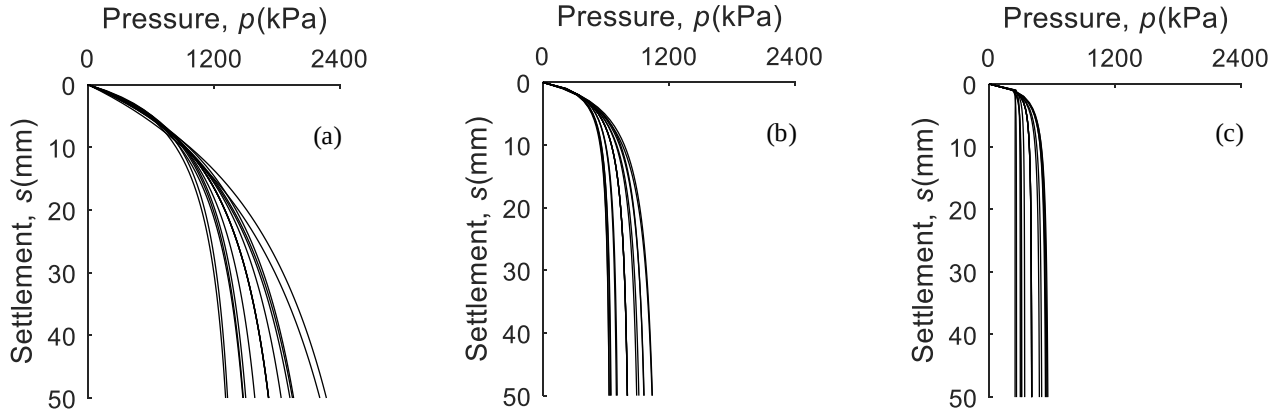

Fig. 4 Relationship between pressure and settlement of the center at the bottom of the footing after (a) 1st iteration, (b) 2nd iteration and (c) 5th iteration (The pressure corresponds to the settlement s_a = 50 mm represents the bearing capacity estimated from each *p-s* curve)

Accordingly, a horizontal ACD of L_h = 30 m and vertical ACD of L_v = 3 m is considered as the basic computation condition. Furthermore, four more values of horizontal ACDs (L_h = 6, 9, 12, and 15 m) and one more value of vertical ACD (L_v = 1 m) are considered for investigating the influence of ACDs on the reliability index of the footing.

3.2 Numerical model and performance function

To estimate the bearing capacity of the strip footing, a plain strain numerical model was set up. The width and height of this numerical model were set to be 5*B* (10 m) and 3*B* (6 m), respectively (Fig. 2(a)). The side length of each discrete element is 0.5 m. The horizontal displacements of nodes on both sides of the numerical model were constrained, and both the horizontal and vertical displacements of nodes at the bottom of this numerical model were constrained. The two vertical sides of this model were impermeable. The initial suction (Ψ_0) in the unsaturated soil was proportional to the vertical distance between the research point and the water level (e.g., as shown in Fig. 2(b), the initial suction at the top of the numerical model is $\gamma_w h_w$ = 98 kPa, where γ_w = 9.8 kN/m^3 is the unit weigh of water. By applying a uniform vertical load at the bottom of a footing through numerical simulation, a relationship between load (p) and settlement (s) of the midpoint at the bottom of the footing can be obtained. Then, the bearing capacity (R) can be computed according to this *p-s* relationship for a given allowable settlement s_a (Fig. 2(c)) (Roberts and Misra 2009, Dithinde *et al.* 2011, Tan *et al.* 2017).

For the shallow strip foundation under rainfall infiltration shown in Fig. 2, the performance function (Z) required in reliability analysis can be expressed as follows:

$$Z = g(\boldsymbol{X}) = R(\boldsymbol{X}) - Q \tag{8}$$

where $R(\boldsymbol{X})$ is the bearing capacity estimated from the numerical simulation; and Q is the load acting at the bottom of the footing. Both $g(\boldsymbol{X})$ and $R(\boldsymbol{X})$ are functions of basic variable $\boldsymbol{X}$. In this example, $\boldsymbol{X}$ represents the two random fields of shear strength parameters (c' and φ'). Therefore, N = 2 in this example. After random discretization using the KL expansion method, the two random fields can be discretized into $n = M \times N = 2M$ standard normal variables, and these variables ($\boldsymbol{X}$ = [X_1, X_2, …X_M, X_{M+1}, …, X_{2M}]) are the basic variables in the traditional FORM algorithm.

The seepage and deformation process under rainfall infiltration was simulated using the finite difference code FLAC (Itasca 2006). A FISH (the built-in programming language of FLAC) function was written for automatically performing the above numerical simulation. As shown in

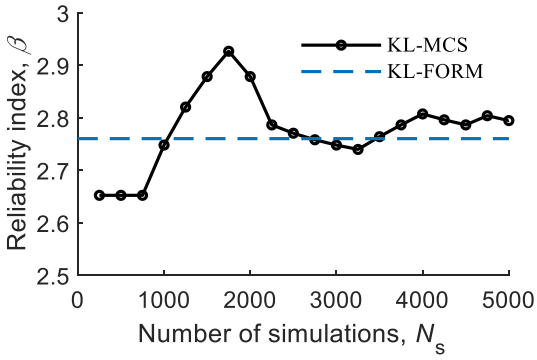

Fig. 5 Relationship between reliability index at the end of rainfall and number of simulations for the KL-MCS (The dashed line represents the reliability index computed by the KL-FORM)

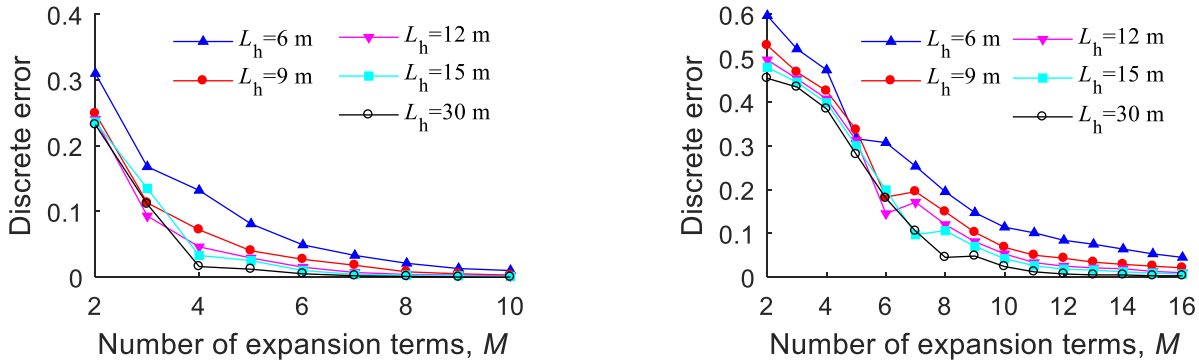

(a) L_v = 3 m (b) L_v = 1 m

Fig. 6 Relationship between the discrete error and the number of series expansion terms for different ACDs

the right column of Fig. 1, the inputs to the FISH function are the realizations of each random field, and the outputs of the FISH function are the values of the performance function, which will be described in Section 3.3. The main code of the KL-FORM algorithm was written in MATLAB.

3.3 Iterative computation for the reliability index at the end of rainfall

According to Eq. (5), the discrete error (ε_d) corresponding to different number of series expansion terms (M) can be estimated for the numerical model of the footing. For the basic computation condition of L_h = 30 m and L_v = 3 m, the computed ε_d for M = 2, 3, 4, and 5 is 23.16%, 11.11%, 1.60% and 1.17%, respectively. Note that ε_d decreases quickly as M increases. When M = 4, the value of ε_d is very small and could be ignored. Therefore, the optimal value of the number of expansion terms is taken as M = 4.

The iterative process for the reliability index of the strip footing at the end of the rainfall for the basic computation condition (i.e., L_h = 30 m and L_v = 3 m) is listed in Table 2. After five iterative computations, the design points become closer and closer, and the reliability indices tend to be stable. The reliability index for this strip footing at the end of rainfall is β = 2.76.

As mentioned in Section 2.2, when the number of expansion terms is M = 4 and the number of random fields is N = 2, the number of discrete random variables is $n = MN$ = 8, and the sample points needed in each iteration of the KL-FORM algorithm is $N_s = 2n+1 = 17$. Then, for each sample point, the two random fields of c' and φ' should be discretized for the computation of the performance function and the gradient of the performance function with respect to basic parameters. For example, the discrete random fields for c' and φ' for the design point of the last iterative computation are shown in Fig. 3, in which the color from dark to light specifies small to large values. After the two random fields of c' and φ' were discretized for the N_s = 17 sample points, numerical analysis was carried out to calculate the values of Z and $\partial Z/\partial X_i$ (i = 1, 2, …, 8). The 17 p–s curves for the 1st, 2nd, and 5th iterations of the KL-FORM algorithm, as computed by the numerical analyses, are shown in Fig. 4. This shows that the 17 p–s curves for the 1st iteration in Fig. 4(a) are relatively scattered compared with those of Figs. 4(b) and 4(c). With the increase of the iterative number, the 17 p–s curves become closer and closer. The p–s curves of the 3rd and 4th iterations are similar to those of the 5th iteration, so the formers are not shown in Fig. 4.

As listed in Table 2, 85 sample points are required for the iterative computations of reliability indices. This implies that only 85 discretization of random fields and numerical simulations are required to obtain a stable reliability index using the KL-FORM algorithm. The runtimes on a computer with a Core i7 CPU @ 3.60 GHz and 24.0 GB of RAM for each iteration are shown in the rightmost column in Table 2. The total runtime is 91.08 seconds to calculate

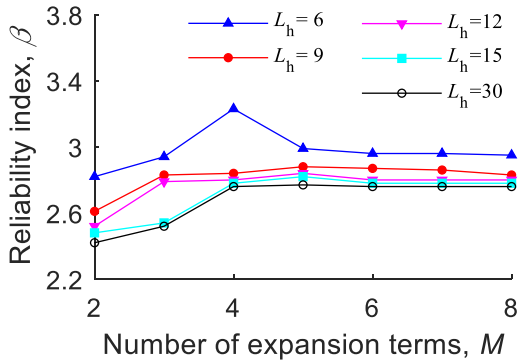

(a) L_v = 3 m

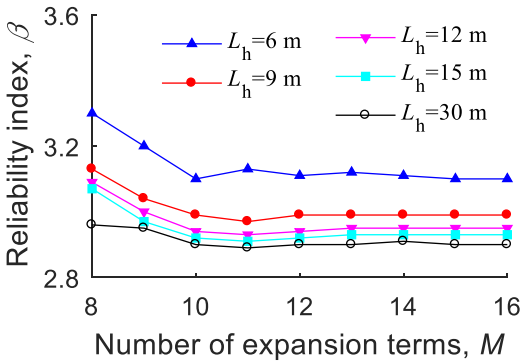

(b) L_v = 1 m

Fig. 7 Relationship between the reliability index and the number of series expansion terms for different ACDs

Table 3 Optimal value of the number of series expansion terms (M) for different ACDs

L_h (m)	6	9	12	15	30
M for L_v=3 m	6	5	4	4	4
M for L_v=1 m	16	12	11	10	10

Table 4 Total number of numerical simulations (n_T) for different ACDs

L_h (m)	6	9	12	15	30
n_T for L_v=3 m	125	105	85	85	85
n_T for L_v=1 m	325	245	225	205	205

the reliability index for the basic computation condition.

3.4 Computational accuracy and efficiency of the KL-FORM

To validate the computational accuracy and efficiency of the KL-FORM, the direct MCS is used for the reliability analysis of the strip footing. Under the basic computation condition, the relationship between the reliability index for this strip footing at the end of rainfall and the number of simulations using the KL-MCS is presented in Fig. 5. This indicates that the reliability index of the KL-MCS varies around the reliability index of the KL-FORM after more than 2,000 MCSs, and the β-N_S curve has not yet stabilized after 5,000 simulations. It can be reasonably inferred that the number of simulations required for the KL-MCS to reach a stable value of the reliability index is very large compared to that of the KL-FORM. This comparison means that the proposed KL-FORM is not only accurate but also computationally efficient.

To further validate the computational accuracy and efficiency of the KL-FORM, the discrete error and the reliability index at the end of rainfall for the strip foundation were computed for different number of series expansion terms and different ACDs. The ε_d-M relationship for different ACDs are shown in Fig. 6, and the corresponding β-M relationship are shown in Fig. 7.

Fig. 6 shows that the discrete error decreases quickly as the number of series expansion terms increases, and the discrete error increases as the vertical ACD decreases. Based on each curve in Fig. 6, the number of series expansion terms with a discrete error closest to but smaller than ε_{d0} = 5% is selected as the optimal value of the number of expansion terms, which are listed in Table 3 for different ACDs.

The optimal value of the number of expansion terms can be further verified by the β–M relationship shown in Fig. 7. For the case of L_v = 3 m (Fig. 7(a)), all curves vary greatly when M < 4, and these curves become stable with the increase of M. The optimal values of M for L_h = 6, 9, 12, 15, and 30 m are 6, 5, 4, 4, and 4, respectively. These optimal values of M are the same as those listed in Table 3, which are obtained by the ε_d-M relationship shown in Fig. 6(a). Similar corresponding relationship can be found from Fig. 6(b), Fig. 7(b), and Table 3 for L_v = 1 m. The consistency demonstrates that the selection of the optimal value of expansion terms based on the ε_d-M relationship is reasonable.

It should be mentioned that the β-M relationship shown in Fig. 7 is only used for demonstrating the computational accuracy of the proposed KL-FORM. It's not needed for the selection of the optimal value of expansion terms because the calculation of reliability index involves numerical simulations, which are much more time-consuming than the calculation of the discrete error. The selection of the optimal value of expansion terms can be easily and quickly determined by the ε_d-M relationship.

Similar to the iterative process listed in Table 2, our computation shows that the reliability index converges after five iterations for all ACDs for the case study of the strip footing. Then, the total number of numerical simulations (n_T) in each reliability analysis using the KL-FORM algorithm is $5N_s = 5(2MN+1) = 5(4M+1)$. Based on the optimal values of expansion terms for different ACDs listed in Table 3, the value of n_T for different ACDs can be calculated and they are listed in Table 4. This shows that the number of simulations required in the KL-FORM increases with the decrease of ACDs. The largest number of numerical simulations is 325, which corresponds to the small ACDs of L_h = 6 m and L_v = 1 m. This number of numerical simulations is still far less than those required by the MCS. The numbers of simulations listed in Table 4 are also very small even compared with the advanced MCS method of subset simulation and probabilistic collocation

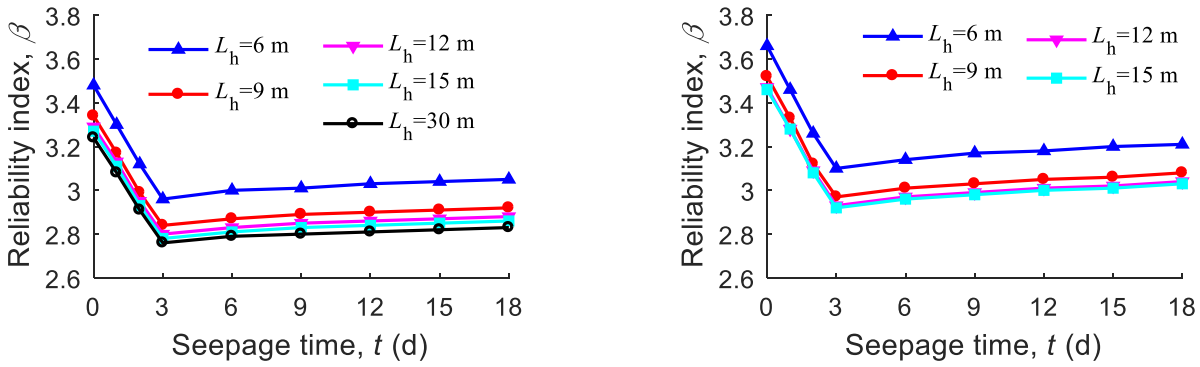

(a) L_v = 3 m (b) L_v = 1 m

Fig. 8 Relationship between reliability index and seepage time for different ACDs

method because these methods need at least several thousands of simulations (Li *et al.* 2009, Santoso *et al.* 2011, Ahmed and Soubra 2014, Jiang *et al.* 2014, Papaioannou *et al.* 2015, Jiang and Huang 2016, Li *et al.* 2016, Liu *et al.* 2017).

3.5 Influence of the ACD on the reliability index

Benefiting from the computational accuracy and efficiency of the KL-FORM, we can easily and quickly perform multiple reliability analyses under different conditions. Fig. 8 shows the reliability index (β) versus seepage time (t) relationship for different ACDs. All curves in Fig. 8 reflect a similar relationship between the reliability index and seepage time. The reliability index decreases with seepage time for the first three days and then gradually increases with seepage time. This occurs because during the first three days of rainfall, the suction of the unsaturated soil is reduced due to the infiltration of rainfall, which consequently results in the decrease of shear strength of the unsaturated soil. This decreases the stability of the footing. After the rainfall ceases, some water in the underlying soil of the footing flows downward and the suction in the unsaturated soil recovers gradually. This leads to the slight increase of the reliability index of the footing. These curves also indicate that a stable footing may become unstable due to rainfall, and the stopping time of rainfall is the most dangerous time for a footing to be built in unsaturated soil under rainfall. Engineers should consider this situation when assessing the stability of a footing.

Fig. 8 also shows that a larger ACD corresponds to a smaller reliability index. For example, the curves in both Fig. 8(a) and Fig. 8(b) drops with the increase of horizontal ACD; and for the same seepage time and horizontal ACD, the reliability indices in Fig. 8(a) are smaller than their corresponding values in Fig. 8(b). The largest difference appears between the curves of L_h = 6 m and L_h = 9 m in both Fig. 8(a) and Fig. 8(b). The difference between two adjacent curves becomes smaller when the horizontal ACD increases. For the case of L_v = 1 m, the β–t curves with L_h = 12 m and 15 m almost overlap (Fig. 8(b)), which indicates that the reliability index has become stable with the increase of L_h. This phenomenon indicates that the horizontal ACD has a relatively large influence on the reliability index of the

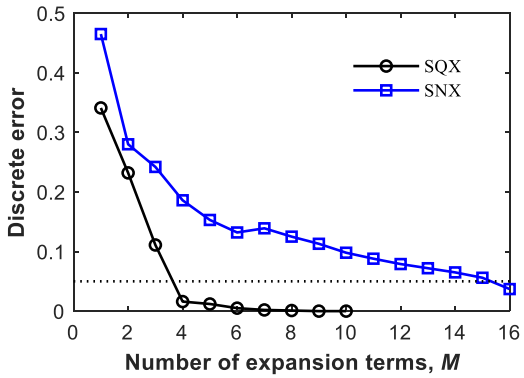

Fig. 9 Relationship between discrete error and number of series expansion terms for different ACFs with L_h=30 m and L_v=3 m

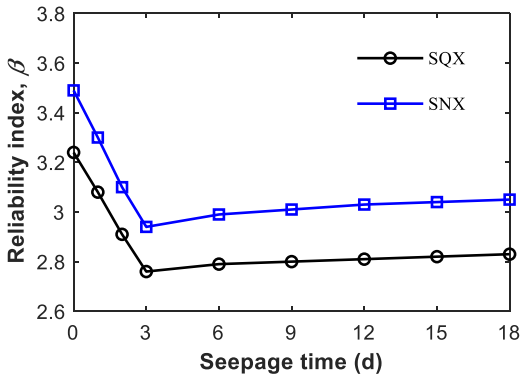

Fig. 10 Relationship between reliability index and seepage time for different ACFs with L_h=30 m and L_v=3 m

footing when the horizontal ACD is relatively small. Not considering the spatial variability of soils (which means considering the ACD to be infinite) will lead to an underestimation of the reliability index of the footing. This will lead to a conservative design of a footing.

Because the horizontal ACD (L_h) has a relatively large influence on the reliability index of the footing when L_h is small, the sampling distance for measuring the L_h should be carefully designed for field test. In general, the measured ACD is larger than the distance between two adjacent sampling points (Firouzianbandpey *et al.* 2014). Therefore,

the sampling points should be dense enough in the horizontal direction. Otherwise, the horizontal ACD will be overestimated, which will lead to an underestimation of the reliability index of the footing.

3.6 Influence of ACF on the reliability index

To investigate the influence of ACF to the reliability index of the footing, the SNX (see Eq. (2)) is considered as the ACF for the basic computation condition of L_h=30 m and L_v=3 m. Fig. 9 shows the relationship between the discrete error and the number of series expansion terms for the SQX and SNX. The horizontal line represents the allowable discrete error (ε_{d0}) of 5%. It is apparent that the discrete error corresponding to SNX is much larger than those of SNX. The optimal number of series expansion terms for the SQX is M=16, while the optimal number of series expansion terms for the SQX is M=4. The computation using the KL-FORM show that the total number of numerical simulations in the KL-FORM is 365 for the SNX. This number is larger than the corresponding value of 85 for the SQX, but it is still much less than those of the MCS, which needs at least several thousands of numerical simulations to obtain a stable value of reliability index.

The relationship between the reliability index (β) and seepage time (t) for the two ACFs of SQX and SNX are shown in Fig. 10. The shapes of these two lines are similar. This indicates that the proposed KL-FORM can be correctly used for different types of ACF. Under the same computational condition, the reliability index of the SNX is larger than those of the SQX, which represents that using the SNX as the ACF will result in overestimating of the reliability index of the footing.

4. Conclusions

The effect of spatial variability of soil parameters on the stability of a strip footing was studied using random field theory. A squared exponential ACF is used to describe the spatial variability of soil parameters. A KL-FORM is proposed to carry out the reliability analysis with consideration of the spatial variability of soil parameters. In the KL-FORM algorithm, the KL expansion is used to discretize random fields, and the FORM is adopted to perform the reliability analysis. By considering the corresponding relationship between the design point $\boldsymbol{x}^*$ in the FORM and the random matrix $\boldsymbol{\xi}$ in the KL expansion, the discretization of random fields and the reliability analysis can be combined to compute the reliability index of footings. Any existing computer programs or software using the FORM can be adopted for the calculation of the reliability index, and any standalone deterministic numerical packages can be adopted to calculate the performance function. Therefore, the KL-FORM is easy to implement.

The case study that considers the spatial variabilities of soil parameters demonstrates that the proposed KL-FORM is computationally accurate and efficient. The results of the KL-FORM show that the reliability index decreases with the increase of ACD. Not considering the spatial variability of soils (e.g., the traditional random variable method that considers the ACD to be infinite) will lead to an underestimation of the reliability index of the footing. For the strip footing under rainfall, the most unstable situation is at the end of rainfall.

Although the case study in this work is a strip footing, the proposed KL-FORM can be easily applied to other geotechnical problems such as reliability analysis of slopes.

Acknowledgments

This work was supported by the National Natural Science Foundation, China (41972278; 41572282). We would like to thank Uni-edit (www.uni-edit.net) for editing and proofreading this manuscript.

References

Ahmed, A. and Soubra, A.H. (2014), "Probabilistic analysis at the serviceability limit state of two neighboring strip footings resting on a spatially random soil", *Struct. Saf.*, **49**, 2-9. http://doi.org/10.1016/j.strusafe.2013.08.001.

Ahmed, A.A. (2009), "Stochastic analysis of free surface flow through earth dams", *Comput. Geotech.*, **36**(7), 1186-1190. https://doi.org/10.1016/j.compgeo.2009.05.005.

Al-Bittar, T., Soubra, A.H. and Thajeel, J. (2018), "Kriging-based reliability analysis of strip footings resting on spatially varying soils", *J. Geotech. Geoenviron. Eng.*, **144**(10), 04018071. http://doi.org/10.1061/(ASCE)GT.1943-5606.0001958.

Cheon, J.Y. and Gilbert, R.B. (2014), "Modeling spatial variability in offshore geotechnical properties for reliability-based foundation design", *Struct. Saf.*, **49**, 18-26. https://doi.org/10.1016/j.strusafe.2013.07.008.

Cho, S.E. and Park, H.C. (2010), "Effect of spatial variability of cross-correlated soil properties on bearing capacity of strip footing", *Int. J. Numer. Anal. Meth. Geomech.*, **34**(1), 1-26. https://doi.org/10.1002/nag.791.

Deodatis, G. (1991), "Weighted integral method I: Stochastic stiffness matrix", *J. Eng. Mech.*, **117**(8), 1851-1864. https://doi.org/10.1061/(ASCE)0733-9399(1991)117:8(1851).

Dithinde, M., Phoon, K.K., Wet, M.D. and Retief, V. (2011), "Characterization of model uncertainty in the static pile design formula", *J. Geotech. Geoenviron. Eng.*, **137**(1), 70-85. https://doi.org/10.1061/(ASCE)GT.1943-5606.0000401.

Duncan, J.M. (2000), "Factors of safety and reliability in geotechnical engineering", *J. Geotech. Geoenviron. Eng.*, **126**(4), 307-316. https://doi.org/10.1061/(ASCE)1090-0241(2000)126:4(307).

Fei S.Z., Tan X.H., Wang X., Du L.F. and Sun Z.H. (2019), "Evaluation of soil spatial variability by micro-structure simulation", *Geomech. Eng.*, **17**(6), 565-572. https://doi.org/10.12989/gae.2019.17.6.565.

Firouzianbandpey, S., Griffiths, D.V. and Andersen, L.V. (2014), "Spatial correlation length of normalized cone data in sand: Case study in the north of Denmark", *Can. Geotech. J.*, **51**(8), 844-857. https://doi.org/10.1139/cgj-2013-0294.

Fredlund, D.G. and Houston, S.L. (2009), "Protocol for the assessment of unsaturated soil properties in geotechnical engineering practice", *Can. Geotech. J.*, **46**(6), 694-707. http://doi.org/10.1139/T09-010.

Gong, W., Juang, C.H. and Martin, J.R. (2016), "A new framework for probabilistic analysis of the performance of a supported excavation in clay considering spatial variability", *Géotechnique*, **67**(6), 546-552. https://doi.org/10.1680/jgeot.15.P.268.

Gong, W.P., Juang, C.H., Martin, J.R., Tang, H.M., Wang, Q.Q.

and Huang, H.W. (2018), "Probabilistic analysis of tunnel longitudinal performance based upon conditional random field simulation of soil properties", *Tunn. Undergr. Sp. Tech.*, **73**, 1-14. https://doi.org/10.1016/j.tust.2017.11.026.

Gravanis, E., Pantelidis, L. and Griffiths, D.V. (2014), "An analytical solution in probabilistic rock slope stability assessment based on random fields", *Int. J. Rock Mech. Min. Sci.*, **71**, 19-24. https://doi.org/10.1016/j.ijrmms.2014.06.018.

Gui, S.X., Zhang, R.D. and Xue, X.Z. (2000), "Probabilistic slope stability analysis with stochastic soil hydraulic conductivity", *J. Geotech. Geoenviron. Eng.*, **136**(1), 1-9. https://doi.org/10.1061/(ASCE)1090-0241(2000)126:1(1).

Itasca (2006), *Reference Manual, FLAC 5.0. Minneapolis*, Itasca Consulting Group Inc, Minnesota, U.S.A.

Jha, S.K. and Ching, J. (2013), "Simulating spatial averages of stationary random field using the fourier series method", *J. Eng. Mech.*, **139**(5), 594-605. https://doi.org/10.1061/(ASCE)EM.1943-7889.0000517.

Ji, J. and Kodikara, J.K. (2015), "Efficient reliability method for implicit limit state surface with correlated non-Gaussian variables", *Int. J. Numer. Anal. Meth. Geomech.*, **39**, 1898-1911. http://doi.org/10.1002/nag.2380.

Ji, J., Liao, H.L. and Low, B.K. (2012), "Modeling 2-D spatial variation in slope reliability analysis using interpolated autocorrelations", *Comput. Geotech.*, **40**(3), 135-146. http://doi.org/10.1016/j.compgeo.2011.11.002.

Ji, J., Zhang, C.S., Gao, Y.F. and Kodikara, J. (2018), "Effect of 2D spatial variability on slope reliability: A simplified FORM analysis", *Geosci. Front.*, **9**, 1631-1638. https://doi.org/10.1016/j.gsf.2017.08.004.

Jiang, S.H. and Huang, J.S. (2016), "Efficient slope reliability analysis at low-probability levels in spatially variable soils", *Comput. Geotech.*, **75**, 18-27. https://doi.org/10.1016/j.compgeo.2016.01.016.

Jiang, S.H., Li, D.Q., Zhang, L.M. and Zhou, C.B. (2014), "Slope reliability analysis considering spatially variable shear strength parameters using a non-intrusive stochastic finite element method", *Eng. Geol.*, **168**, 120-128. https://doi.org/10.1016/j.enggeo.2013.11.006.

Laloy, E., Rogiers, B., Vrugt, J.A., Mallants, D. and Jacques, D. (2013), "Efficient posterior exploration of a high-dimensional groundwater model from two-stage MCMC simulation and polynomial chaos expansion", *Water Resour. Res.*, **49**(5), 2664-2682. https://doi.org/10.1002/wrcr.20226.

Le, T.M.H., Gallipoli, D., Sánchez, M. and Wheeler, S. (2015), "Stability and failure mass of unsaturated heterogeneous slopes", *Can. Geotech. J.*, **52**(11), 1747-1761. https://doi.org/10.1139/cgj-2014-0190.

Li, D.Q., Xiao, T., Cao, Z.J., Zhou, C.B. and Zhang, L.M. (2016), "Enhancement of random finite element method in reliability analysis and risk assessment of soil slopes using Subset Simulation", *Landslides*, **13**, 293-303. http://doi.org/10.1007/s10346-015-0569-2.

Li, W.X., Lu, Z.M. and Zhang, D.X. (2009), "Stochastic analysis of unsaturated flow with probabilistic collocation method", *Water Resour. Res.*, **45**, W08425. http://doi.org/10.1029/2008WR007530.

Liu, L.L., Cheng, Y.M. and Zhang, S.H. (2017), "Conditional random field reliability analysis of a cohesion-frictional slope", *Comput. Geotech.*, **82**, 173-186. https://doi.org/10.1016/j.compgeo.2016.10.014.

Lombardi M., Cardarilli M. and Raspa G. (2017), "Spatial variability analysis of soil strength to slope stability assessment", *Geomech. Eng.*, **12**(3), 483-503. https://doi.org/10.12989/gae.2017.12.3.483.

Montoya-Noguera, S., Zhao, T.Y., Hu, Y., Wang, Y. and Phoon, K.K. (2019), "Simulation of non-stationary non-Gaussian random fields from sparse measurements using Bayesian compressive sampling and Karhunen-Loève expansion", *Struct. Saf.*, **79**, 66-79. https://doi.org/10.1016/j.strusafe.2019.03.006.

Moshtaghin, A.F., Franke, S. and Keller, T. (2016), "Vassilopoulos AP. Random field-based modeling of size effect on the longitudinal tensile strength of clear timber", *Struct. Saf.*, **58**, 60-68. https://doi.org/10.1016/j.strusafe.2015.09.002.

Mouyeaux, A., Carvajal, C., Bressolette, P., Peyras, L., Breul, P. and Bacconnet, C. (2018), "Probabilistic stability analysis of an earth dam by stochastic Finite Element Method based on field data", *Comput. Geotech.*, **101**, 34-47. https://doi.org/10.1016/j.compgeo.2018.04.017.

Papaioannou, I., Betz, W., Zwirglmaier, K. and Straub, D. (2015), "MCMC algorithms for subset simulation", *Probabilist. Eng. Mech.*, **41**, 89-103. http://doi.org/10.1016/j.probengmech.2015.06.006.

Phoon, K.K. and Kulhawy, F.H. (1999), "Characterization of geotechnical variability", *Can. Geotech. J.*, **36**(4), 612-624. https://doi.org/10.1139/t99-038.

Phoon, K.K., Huang, H.W. and Quek, S.T. (2005), "Simulation of strongly non-Gaussian processes using Karhunen-Loeve expansion", *Probabilist. Eng. Mech.*, **20**(2), 188-198. https://doi.org/10.1016/j.probengmech.2005.05.007.

Phoon, K.K., Huang, S.P. and Quek, S.T. (2002), "Implementation of Karhunen-Loeve expansion for simulation using a wavelet-Galerkin scheme", *Probabilist. Eng. Mech.*, **17**(3), 293-303. https://doi.org/10.1016/S0266-8920(02)00013-9.

Phoon, K.K., Quek, S.T. and Huang, H.W. (2004), "Simulation of non-Gaussian processes using fractile correlation", *Probabilist. Eng. Mech.*, **19**(4), 287-292. https://doi.org/10.1016/j.probengmech.2003.09.001.

Qi S.C., Vanapalli S.K., Yang X.G., Zhou J.W. and Lu G.D. (2019), "Stability analysis of an unsaturated expansive soil slope subjected to rainfall infiltration", *Geomech. Eng.*, **19**(1), 1-9. https://doi.org/10.12989/gae.2019.19.1.001.

Rackwitz, R. (2000), "Reviewing probabilistic soils modelling", *Comput. Geotech.*, **26**(3-4), 199-223.

Roberts, L.A. and Misra. A. (2009), "Reliability-based design of deep foundations based on differential settlement criterion", *Can. Geotech. J.*, **46**(2), 168-176. https://doi.org/10.1139/T08-117.

Sachdeva, S.K., Nair, P.B. and Keane, A.J. (2007), "On using deterministic FEA software to solve problems in stochastic structural mechanics", *Comput. Struct.*, **85**(5-6), 277-290. https://doi.org/10.1016/j.compstruc.2006.10.008.

Santoso, A.M., Phoon, K.K. and Quek, S.T. (2011), "Effects of soil spatial variability on rainfall-induced landslides", *Comput. Struct.*, **89**(11-12), 893-900. https://doi.org/10.1016/j.compstruc.2011.02.016.

Schueller, G.L. and Jensen, H.A. (2008), "Computational methods in optimization considering uncertainties – an overview", *Comput. Method. Appl. M.*, **198**(1), 2-13. https://doi.org/10.1016/j.cma.2008.05.004.

Stefanou, G. (2009), "The stochastic finite element method-Past present and future", *Comput. Method. Appl. M.*, **198**(9-12), 1031-1051. https://doi.org/10.1016/j.cma.2008.11.007.

Sudret, B. and Der Kiureghian, A. (2000), "Stochastic finite element methods and reliability", Technical Report No. UCB-SEMM-2000-08; Mechanics and Materials Department of Civil & Environmental Engineering, University of California, California, U.S.A.

Tan, X.H. and Wang, J.G. (2009), "Finite element reliability analysis of slope stability", *J. Zhejiang Univ. Sci. A*, **10**(5), 645-652. http://doi.org/10.1631/jzus.A0820542.

Tan, X.H., Wang, X., Khoshnevisan, S., Hou, X.L. and Zha, F.S. (2017), "Seepage analysis of earth dams considering spatial variability of hydraulic parameters", *Eng. Geol.*, **228**, 260-269.

https://doi.org/10.1016/j.enggeo.2017.08.018.
Tan, X.H., Xie, Y., Hou, X.L., Li, P. and Wang, X. (2017), "Reliability analysis of shallow foundations on unsaturated soils under rainfall infiltration", *Proceedings of the Geo-Risk 2017*, Denver, Colorado, U.S.A., June.
van Genuchten, M.T. (1980), "A closed form equation for predicting the hydraulic conductivity of unsaturated soils", *Soil Sci. Soc. Am. J.*, **44**(5), 892-898. http://doi.org/10.2136/sssaj1980.03615995004400050002x.
Vanmarcke, E. and Grigoriu, M. (1983), "Stochastic finite element analysis of simple beams", *J. Eng. Mech.*, **109**, 1203-1214. https://doi.org/10.1061/(ASCE)0733-9399(1983)109:5(1203).
Vanmarcke, E.H. (1977), "Probabilistic modeling of soil profiles", *J. Geotech. Eng. Div.*, **103**, 1227-1246.
Zhang, J. and Ellingwood, B. (1994), "Orthogonal series expansions of random fields in reliability analysis", *J. Eng. Mech.*, **120**, 2660-2677. https://doi.org/10.1061/(ASCE)0733-9399(1994)120:12(2660).

IC